ELSEVIER

Ceramics International 33 (2007) 497–503

CERAMICS INTERNATIONAL

www.elsevier.com/locate/ceramint

Fabrication and properties of the Nb doped Zr-rich lead zirconate titanate ceramics by a heterogenous precipitation method

Hong Yang [a,*], Alfred Lyashchenko [b], Xian-lin Dong [a], Cai-hong Luo [c], Chao-liang Mao [a], Shu-tao Chen [a], Tao Zeng [a], Yong-ling Wang [a]

[a] *Shanghai Institute of Ceramics, Chinese Academy of Sciences, 1295 Ding-Xi Road, Shanghai 200050, PR China*
[b] *Frantsevich Institute for Problems Materials Science, Ukrainian Academy of Sciences, Kiev 01030, Ukraine*
[c] *Chongqing Environment Monitoring Centre, Chongqing 400020, PR China*

Received 6 June 2005; received in revised form 9 September 2005; accepted 17 October 2005
Available online 20 January 2006

Abstract

A novel heterogenous precipitation method (H-P) combining the merits of solid state synthesis (S-S-S) and the liquid routes was developed to synthesize ZrO_2 phase-free Nb doped Zr-rich PZT ceramics. The microstructure of the ceramics synthesized by H-P was more homogeneous and fine than for S-S-S. The density and the ferroelectric properties of the ceramics synthesized by H-P were higher than that by S-S-S. The dissipation factor tgδ synthesized by H-P was lower than that by S-S-S. The Weibull distribution analysis shows that the dielectric breakdown of the ceramics synthesized by H-P method is markedly improved.

Keywords: C. Ferroelectric properties; D. PZT; Heterogenous precipitation method; Microstructure

1. Introduction

Solid solutions of lead zirconate titanate (PZT) ceramics are known as some of the most useful piezoelectric, ferroelectric and pyroelectric materials. There exits a ferroelectric (FE) and anti-ferroelectric (AFE) phase boundary for a Zr/Ti ratio = 95/5 [1,2]. In a certain range near the FE and AFE phase boundary, the FE phase and the AFE phase can co-exist. This kind of Zr-rich PZT ceramics has gained technical applications for its high-density energy storage and high-density power output [3–8]. Nevertheless, the relative low dielectric breakdown (E_b) and reliability are still a great disadvantage for applications of Zr-rich PZT ceramics. Because both uniform microstructures and high density are important to ceramics with excellent properties and high E_b [9,13]. Therefore, the present trend is to make such materials and devices with uniform microstructures and high density.

In the process of S-S-S, lead titanate is the first reaction product to appear before the PZT solid solution is formed because of the higher diffusion coefficients of Pb^{2+} and Ti^{4+} compared to Zr^{4+} [10]. Therefore, PZT grains show a gradient of Zr/Ti concentration from the core to the shell and the properties of materials are sensitive to the Zr/Ti ratio. It is obvious that the homogenous distribution of Ti^{4+} is important for the properties and microstructure of PZT ceramics [10,11]. A traditional S-S-S method cannot afford the homogenous distribution of Ti^{4+}. Compared to S-S-S method, powders prepared by hydroxide coprecipitation are more homogeneous and reactive. However, almost every wet chemistry-based processing routes require the precursor powders to be calcined in a temperature range of 600–900 °C in order to develop the designed PZT phase. This often results in particle agglomerates in the resulting powder. The presence of these hard particle agglomerates will significantly reduce the sinterability of the powder compact and lead to microstructural defects in the sintered PZT ceramics [13]. The powders prepared by the sol–gel process are more homogeneous and fine. But a Lead excess of 2–12 at.% has to be used to enhance the crystallization of the perovskite phase and to compensate for PbO evaporation [14]. Besides, the cost of sol–gel process is higher than other methods, which is an obvious drawback for mass production. So a novel H-P method combining the merits of S-S-S and the liquid route was recently developed. The objective of the present work is to investigate the effect of different powder

* Corresponding author. Tel.: +86 21 52411512; fax: +86 21 62513903.
E-mail address: t_yhong@yahoo.com.cn (H. Yang).

0272-8842/$32.00
doi:10.1016/j.ceramint.2005.10.020

Table 1
Purities and manufacturers of the starting materials

The starting material	Purity	Manufacturer
Nb_2O_5	Nb_2O_5	Shanghai Yuelong Chemical Plant, China
NH_4OH	21–22% NH_3	Shanghai No. 4 Reagent & H.V. Chemical Co., Ltd., China
Pb_3O_4	97.33%	Shanghai Longrun Chemical Plant, China
TiO_2	98.42%	Shanghai Hengxin Reagent Co., Ltd., China
ZrO_2	99.09%	Jieshui Reagent Co., Ltd., Jiangxi Province, China
$Ti(SO_4)_2$	96%	Nanhuipengyingzhen Chemical Plant, China

processing routes on the microstructure and the properties of PZT ceramics by comparing the S-S-S with the H-P method.

2. Experiments

The composition of material is $PbZr_{0.965}Ti_{0.035}O_3$ + 1 wt.% Nb_2O_5. Starting materials used in this study were Nb_2O_5, NH_4OH, Pb_3O_4, TiO_2, ZrO_2, $Ti(SO_4)_2$. The purities and the manufacturers of the starting materials are listed in Table 1. For preparing $TiO(NO_3)_2$ solution, $Ti(SO_4)_2$ was dissolved in aqueous solution and precipitated by NH_4OH solution. After washed with water for several times, $Ti(OH)_4$ precipitate was reacted by HNO_3 to form a 0.1 mol dm^{-3} $TiO(NO_3)_2$ solution. The reaction was shown in the following equation:

$$Ti(SO_4)_2 + 4NH_4OH \rightleftharpoons Ti(OH)_4\downarrow + 2(HN_4)_2SO_4 \quad (1)$$

$$Ti(OH)_4 + 2HNO_3 \rightleftharpoons TiO(NO_3)_2 + 2H_2O \quad (2)$$

The detailed scheme of the H-P method process was given in Fig. 1. The starting solid powders ZrO_2, Pb_3O_4, Nb_2O_5 and

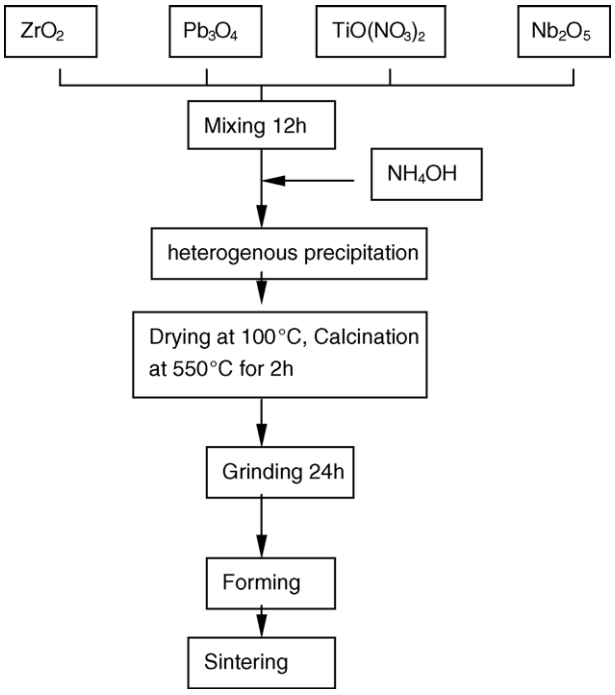

Fig. 1. Flow chart of heterogenous precipitation method.

liquid $TiO(NO_3)_2$ were mixed in a polyethylene pot for 12 h using distilled water and ZrO_2 balls as the grinding medium. Then NH_4OH solution of 1 M was added to the homogeneous slurry obtained above under vigorous stirring. The $TiO(NO_3)_2$ formed $Ti(OH)_4$ precipitate, which dispersed homogeneously in the slurry. The corresponding equation is:

$$TiO(NO_3)_2 + 4NH_4OH \rightleftharpoons Ti(OH)_4\downarrow + 2NH_4NO_3 + 2NH_3\uparrow + H_2O \quad (3)$$

In order to ensure the reaction finished completely, an excess of NH_4OH was added in the slurry and pH value of mixture was

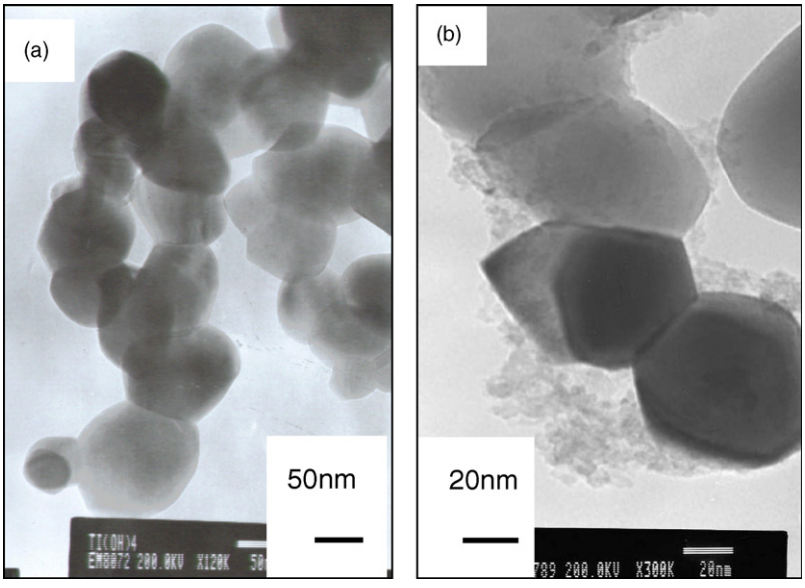

Fig. 2. TEM particles images of the S-S-S method (a) and the H-P method (b).

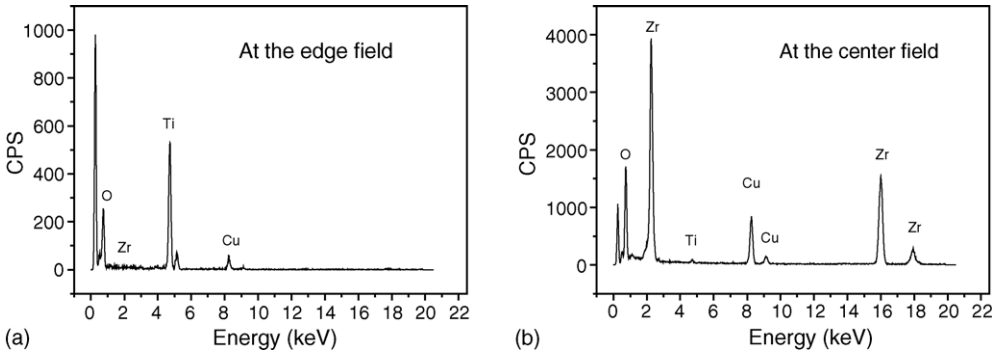

Fig. 3. EDS spectra of the coated particles at the edge field (a) and the center field (b).

kept at 9–10 [12]. The dried powder was heated at 550 °C to decompose the $Ti(OH)_4$ precipitate into TiO_2 [13]. The calcined powder was ball-milled for 24 h again. After drying, the powders were pressed into discs (Ø 17 mm × 2 mm). The materials were sintered at different temperatures (1260–1360 °C) for about 1.5 h in an atmosphere controlled by the same sintered ceramic powder in double high-purity alumina crucibles. Powders and ceramics of $Pb(Zr_{0.965}Ti_{0.035}O_3)$ + 1 wt.% Nb_2O_5 were also prepared by the S-S-S, which experienced a synthesis process at 850 °C and an excess of 1 wt.% PbO in the starting raw powders mixture.

X-ray diffraction (XRD) patterns of ceramics were obtained using an automated diffractometer (Model Rigaku RAX-10) with Cu Kα1 radiation. The microstructure of the sintered ceramics was analyzed by field emission scanning electron microscope (FESEM) (JSM-6700F, JEOL, Japan). A transmission electron microscope (TEM) with energy dispersive spectroscope (EDS) (Model JEM-200CX) was applied to investigate the microstructure of the powders. The density of the sintered bodies was determined by the Archimedes method. For electrical measurements, Ag-paste was pasted on both sides of the discs and then fired at 650 °C for 30 min. The electroded specimens were poled in silicone oil at 120 °C by applying a dc field of 2.5 kV/mm for 20 min. The piezoelectric constant was measured using a quasi-static d_{33} meter (Model ZJ-3D, Institute of Acoustics, China). The dielectric constants and dielectric loss at 1 kHz were measured by an impedance analyzer (HP4294A). Ferroelectric hysteresis loops at room temperature were investigated based on a ferroelectric apparatus (TF Analyzer 2000, AIXACCT Company). Measurements of dielectric breakdown strength were carried out at room temperature for the samples in silicone oil using a plate tester and all samples have the same dimensions Ø 14 mm × 1 mm. In order to compare the breakdown strength of two kinds of ceramic samples, more than 10 samples of every kind of materials were tested.

3. Results and discussion

3.1. Microstructure of the powders

A TEM image of the precursor powders prepared by S-S-S method is shown in Fig. 2(a). It is observed that the particles have a relative smooth and dense surface. A TEM image of the powders prepared by H-P method is shown in Fig. 2(b). It is obvious that there is a coating layer (about 10–20 nm thickness) on the surface of the particles after heterogenous precipitation process. The EDS spectra of the as-precipitated particles indicate that the intensity ratio of Ti peak to Zr peak at the edge field (Fig. 3(a)) is much higher than that in the center field (Fig. 3(b)). This demonstrates that as-precipitated particles are a typical coated structure. The core particle is ZrO_2 particle and the coating layer is the $Ti(OH)_4$ precipitate. $Ti(OH)_4$ precipitate grow on the surface of ZrO_2 particles to form a 10–20 nm coating layer. So we can assure that the Ti^{4+} was distributed homogeneously at the nanometric scale, which will bring an important effect on the properties and microstructure of the ceramics inevitably.

3.2. Phase characterization and microstructure of ceramics

Fig. 4 shows the XRD patterns of the ceramics synthesized by two methods. It can be seen that Zr-rich PZT phase is obtained by both the H-P method and the S-S-S method and there is a faint ZrO_2 diffraction peak in ceramics synthesized by S-S-S, which denotes that a little second phase (ZrO_2) was separated out because of the volatilization of PbO in the

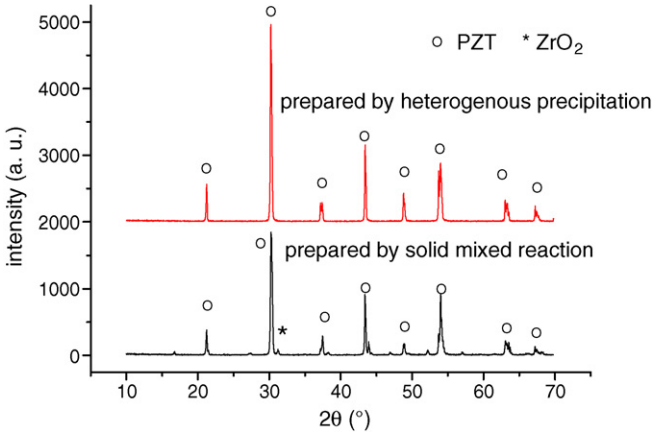

Fig. 4. XRD diagrams of the ceramics synthesized by H-P method and S-S-S method.

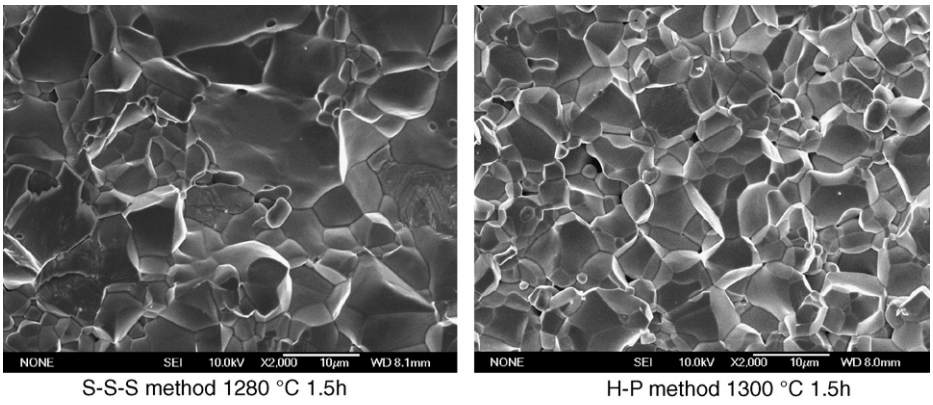

Fig. 5. Microstructure of the ceramics synthesized by two routes.

process. The amount of the perovskite phase is estimated using the following equation:

$$X_{\text{perovskite}\,(\%)} = \left(\frac{I_{(1\,1\,0)\text{perovskite}}}{I_{(1\,1\,0)\text{perovskite}} + I_{(1\,1\,1)\text{ZrO}_2}} \right) \times 100\% \qquad (4)$$

where $I_{(1\,1\,0)\text{perovskite}}$ and $I_{(1\,1\,1)\text{ZrO}_2}$ are the intensity of the (1 1 0) peak of the perovskite phase and the intensity of (1 1 1) peak of the ZrO_2 phase, respectively. By comparing the XRD patterns, we can see that single phase Zr-rich PZT ceramics is synthesized by H-P method. Since no PbO volatilization is assumed in the H-P method which experienced a calcination process at only 550 °C, any excess of PbO do not add in the H-P method. Fig. 5 shows the microstructure of the ceramics synthesized by the two methods. Obviously, the grain size obtained by H-P method is more homogeneous and fine than that by S-S-S.

3.3. Properties of Zr-rich PZT ceramics

Fig. 6 shows the relation between density and sintering temperature of two kinds of ceramics. It can be seen that compact ceramics can be obtained in a wide temperature range from 1280 to 1300 °C with the same sintering time 1.5 h. The density of ceramics synthesized by H-P method is higher than that by S-S-S. Figs. 7 and 8 show the dielectric properties and the dissipation factor of the ceramics synthesized by both two methods, respectively. The Curie temperature and the dissipation factor of the ceramics synthesized by H-P method are lower than that by S-S-S. Fig. 9 shows the ferroelectric

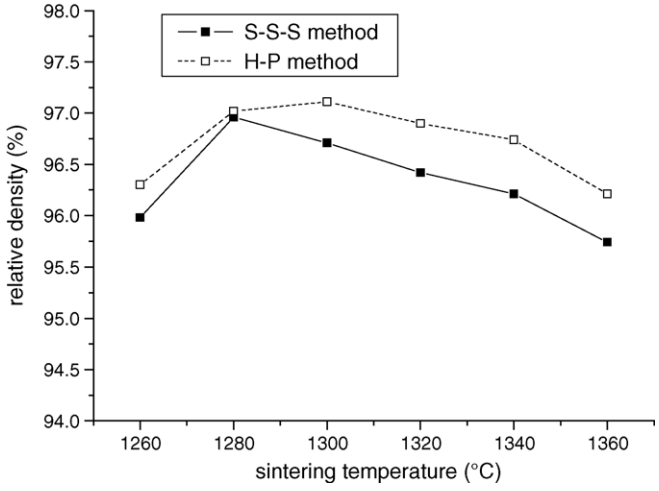

Fig. 6. Curve between density and sintering temperature of Zr-rich PZT ceramics.

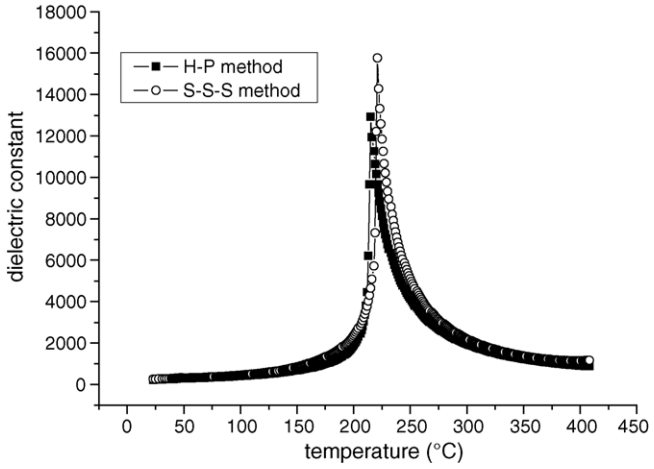

Fig. 7. Dielectric constant of the ceramics synthesized by two routes.

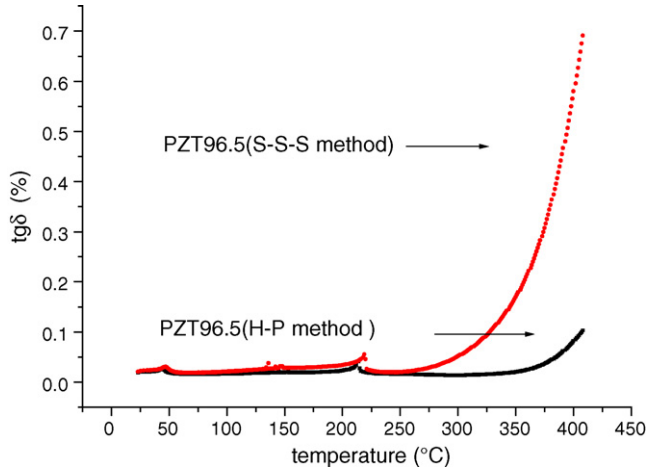

Fig. 8. Dissipation factor of the ceramics synthesized by two routes.

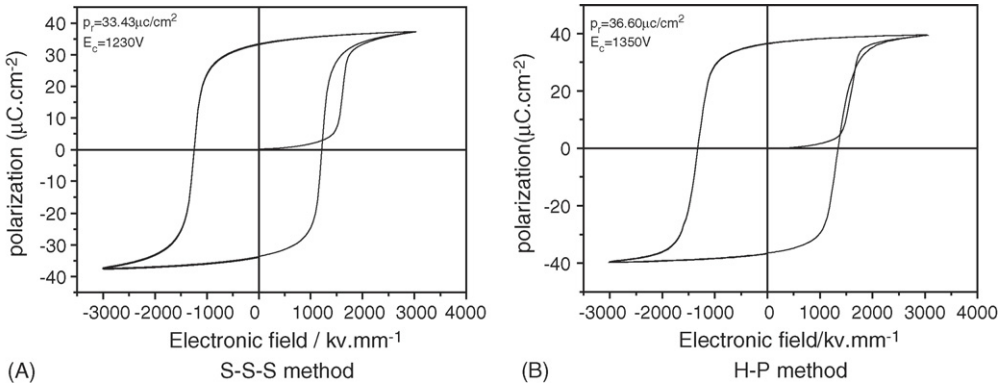

Fig. 9. Hysteresis loops of Nb doped PZT ceramics by two routes.

properties of the ceramics synthesized by two routes. It can be seen that the remnant polarization and the coercive field of the ceramics synthesized by H-P method is slightly higher than that by S-S-S.

3.4. Dielectric breakdown properties of Zr-rich PZT ceramics

Dielectric breakdown property is very crucial for electrical ceramics because the energy density per unit volume of capacitor is dependent on the square of the voltage. A substantial gain in charge storage can be realized if E_b of the dielectric has been improved. Since Weibull distribution was introduced by Weibull, a Sweden physicist in the 1950s, it has become a useful data treatment method in reliability studies of material and electronic devices [15]. The Weibull distribution is applied in studies of not only mechanical failure of ceramics, but also dielectric failure of ceramics, which may imply that the fracture origins in both failures are similar [16]. Tables 2 and 3

Table 2
Weibull distribution analysis to breakdown voltage of ceramic samples by S-S-S method

Number (j)	U_j (kV)	$X_j = \ln(U_j)$	$Y_j = \ln(-\ln(1 - j/(n+1)))$
1	4.8	1.5686	−2.3506
3	5.1	1.6292	−1.1443
5	5.2	1.6486	−0.5007
6	5.3	1.6677	−0.2377
7	5.4	1.6864	0.0115
8	5.6	1.7228	0.2618
9	6.2	1.8245	0.5334
10	6.3	1.8405	0.8746

Table 3
Weibull distribution analysis to breakdown voltage of ceramic samples by H-P method

Number (j)	U_j (kV)	$X_j = \ln(U_j)$	$Y_j = \ln(-\ln(1 - j/(n+1)))$
1	5.7	1.7405	−2.3506
2	5.8	1.7578	−1.6061
3	6.0	1.7918	−1.1443
4	6.1	1.8083	−0.7941
5	6.2	1.8245	−0.5007
6	6.3	1.8405	−0.2377
7	6.4	1.8563	0.0115
8	6.5	1.8718	0.2618
9	6.6	1.8871	0.5334
10	7.2	1.9741	0.8746

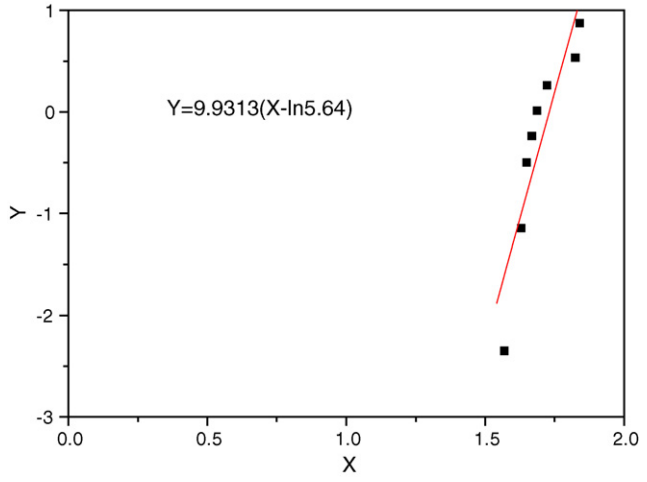

Fig. 10. Weibull probability figure vs. breakdown voltage of Zr-rich PZT ceramics (S-S-S method).

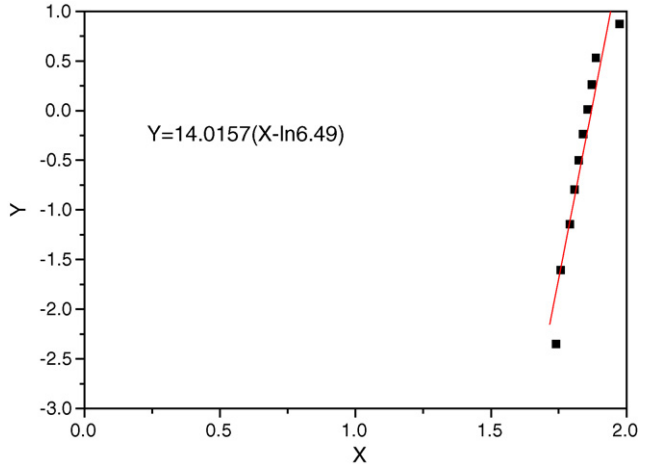

Fig. 11. Weibull probability figure vs. breakdown voltage of Zr-rich PZT ceramics (H-P method).

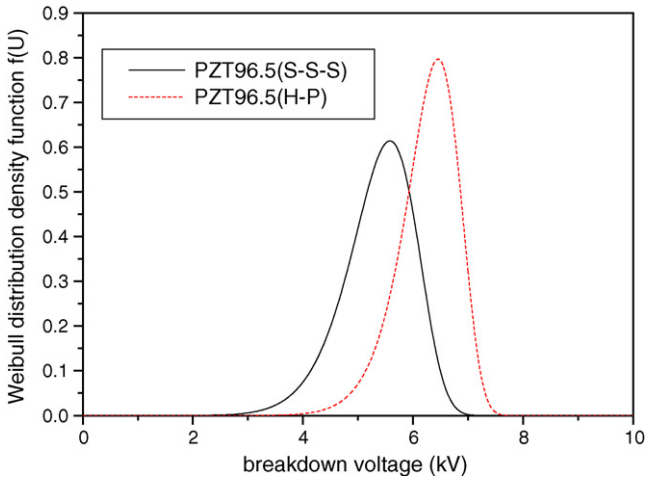

Fig. 12. Weibull distribution density function vs. breakdown voltage.

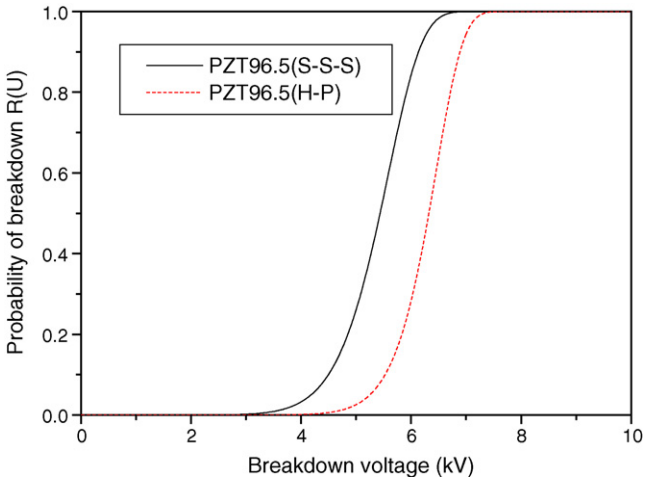

Fig. 13. Probability of breakdown vs. voltage.

list the E_b values of two kinds of samples. In actual data treatment procedures, the data were transformed according to Weibull distribution: $Y_j = \ln(-\ln(1 - j/(n + 1)))$ and $X_j = \ln(U_j)$, where every specific breakdown voltage (U_j) is the swatch, n the sum of swatch, and j is the serial number of swatch. For two parameters (shape parameter β and scale parameter η) Weibull distribution, $Y_j(X_j)$ function should be a line in a coordinate axis, where the slope of the line is shape parameter β and the intercept is the scale parameter η.

Figs. 10 and 11 are Weibull probability figures of breakdown voltage of S-S-S samples and H-P method samples, respectively. It can be seen that both two breakdown data are accorded with Weibull distribution. The shape parameter $\beta = 9.9313$ and scale parameter $\eta = 5.64$ can be deduced for S-S-S samples, respectively. Similar to H-P method samples, the shape parameter β is 14.0157 and scale parameter η is 6.49 for H-P method samples. Having known the shape parameter β and the scale parameter η, we can acquire the Weibull distribution density function ($f(U)$) and the probability of breakdown ($R(U)$) according to the following formula:

$$f(U) = \left(\frac{\beta}{\eta}\right)\left(\frac{U}{\eta}\right)^{\beta-1} \exp\left(-\left(\frac{U}{\eta}\right)^{\beta}\right) \quad (5)$$

$$R(U) = 1 - \exp\left(-\left(\frac{U}{\eta}\right)^{\beta}\right) \quad (6)$$

Figs. 12 and 13 are Weibull distribution density function versus voltage and probability of breakdown versus voltage, respectively. From Fig. 12, it can be observed that the E_b of H-P method samples are more concentrated and higher than that of S-S-S samples. From Fig. 13 we can see that at the same voltage, the breakdown probability of H-P method samples is lower than that of S-S-S samples. So it is clear that the dielectric breakdown properties of H-P method samples are better than that of S-S-S samples.

4. Conclusion

Single phase Zr-rich PZT ceramics were successfully synthesized by the H-P method. Compared to S-S-S and other liquid routes, the H-P method exhibited almost no PbO volatilization. The microstructure of the ceramics synthesized by H-P was more homogeneous and fine than that by S-S-S. The density, the ferroelectric properties and the E_b of ceramics synthesized by H-P are higher than those by S-S-S. The process of H-P can ensure both the chemical homogeneity and the low cost in mass production, which combines the merits of the traditional solid reaction method and the liquid routes.

Acknowledgement

The authors thank for the support from the Great Fundamental Research Project of Science and Technology Commission of Shanghai Municipality (04DZ14002).

References

[1] Z. Ujma, Phase transition in lead–lanthanum zirconate–titanate ceramics with a Zi/Ti ratio of 92/8 and a La content up to 1 at.%, J. Phys. Condens. Matter 7 (1995) 895–906.
[2] D. Viehland, J.-f. Li, X. Dai, Z. Xu, Structural and property studies of high Zr-content lead zirconate titanate, J. Phys. Chem. solids 57 (1996) 1545–1554.
[3] N. Duan, N. Cereceda, B. Noheda, A. Gonzalo, Dielectric characterization of the phase transitions in $Pb_{[1-y/2]}(Zr_{[1-x]}Ti_{[x]})_{[1-y]}Nb_{[y]}O_{[3]}$ ($0.03 \le x \le 0.04$, $0.02 \le y \le 0.05$), J. Appl. Phys. 82 (1997) 779–784.
[4] Y.-L. Wang, W.-Z. Yuan, Study on shock wave-explosive energy converter of PZT95/5 ferroelectric ceramics, Ferroelectrics 49 (1983) 169–176.
[5] S.S.N. Bharadwaja, S. Saha, S. Bhattacharyya, S.B. Krupanidhi, Dielectric properties of La-modified antiferroelectric $PbZrO_3$ thin films, Mater. Sci. Eng. B. 88 (2002) 22–25.
[6] Z. Ujma, L. Szymczak, J. Handerek, K. Szot, H.J. Penkalla, Dielectric and pyroelectric properties of Nb-doped $Pb(Zr_{0.92}Ti_{0.08})O_3$ ceramics, J. Euro. Ceram. Soc. 20 (2000) 1003–1010.
[7] Y.-J. Chang, J.-Y. Lian, Y.-l. Wang, One-dimensional regular arrays of antiphase domain boundaries in anti-ferroelectric tin-substituted lead zirconate titanate (PZT) ceramics, Appl. Phys. A 36 (1985) 221–227.

[8] S. Zhang, X. Dong, S. Kojima, Temperature dependence of dielectric, elastic and piezoelectric properties of $Pb(Zr_xTi_{1-x})O_3$ ceramics near the morphotropic phase boundary, Jpn. J. Appl. Phys. 36 (1997) 2994–2997.

[9] B.A. Tuttle, P. Yang, Pressure-induced phase transformatin of controlled-porosity $Pb(Zr_{0.95}Ti_{0.05})O_3$ ceramics, J. Am. Ceram. Soc. 84 (2001) 1260–1264.

[10] M. Laurent, U. Schreiner, P.A. Langjahr, M.J. Hoffmann, Microstructural and electrical characterization of La-doped PZT ceramics prepared by a precursor route, J. Euro. Ceram. Soc. 21 (2001) 1495–1498.

[11] M. Hammer, M.J. Hoffmann, Sintering model for mixed-oxide-derived lead zirconate titanate ceramics, J. Am. Ceram. Soc. 81 (1998) 3277–3284.

[12] Ch. Jin-Ho, H. Yang-Su, K. Seung-Joo, Oxalate coprecipitation route to the piezoelectric $Pb(ZrTi)O_3$ oxide, J. Mater. Chem. 7 (1997) 1807–1813.

[13] L. Guo, A. Lyashchenko, X.-l. Dong, Synthesis of zirconium-rich PZT ceramics by hydroxide coprecipitation under hot-press, Mater. Lett. 56 (2002) 849–855.

[14] M. Klee, R. Eusemann, R. Waser, W. Brand, Processing and electrical properties of Pb $(Zr[x]Ti[1-x])O[3]$ ($x = 0.2$–0.75) films: comparison of metallo-organic decomposition and sol–gel processes. J. Appl. Phys. 72 (4), 1566–1576.

[15] W. Weibull, A statical distribution of wide applicability, J. Appl. Mech. 18 (1951) 293–302.

[16] A. Kishimoto, K. Koumoto, H. Yanagida, Mechanical and dielectric failure of $BaTiO_3$ ceramics, J. Sci. 24 (1989) 698–702.